Astron. Astrophys. 364, 853–858 (2000)

ASTRONOMY AND ASTROPHYSICS

Special fine structures of solar radio bursts on April 15 1998

Z. Ning[1,2,3], **Q. Fu**[1,3], **and Q. Lu**[2]

[1] Chinese Academy of Sciences, Beijing Astronomical Observatory, Beijing 100012, P.R. China (ningzongjun@hotmail.com)
[2] University of Fudan, Department of Physics, Shanghai 200433, P.R. China
[3] Chinese Academy of Sciences, National Astronomical Observatories, Beijing 100012, P.R. China

Received 9 July 2000 / Accepted 11 August 2000

Abstract. The 2.60–3.80 GHz spectrometer in Beijing Astronomical Observatory (BAO) recorded two remarkable "decimetric pulsation" events (DCIM) around the time 1998 0415 0800 UT. High resolution dynamic spectra revealed various new fine structures during the rising phase of the second DCIM, which seem different from "zebra patterns" well known at lower frequencies. The high frequency limit of the second DCIM is delineated by 1 to 3 narrow and continuous emission bands whose frequencies fluctuate in parallel, and which occasionally split and merge. They look like the "evolving emission line" (EEL) reported by Chernov et al. (1998) at lower frequencies. It is the second time that such a feature has been recorded, and the first time above 1 GHz.

Key words: Sun: activity – Sun: radio radiation

1. Introduction

Observational properties and theoretical aspects of type IV solar radio bursts are much less studied than those of the type III bursts; the observational properties of fine structures in type IV bursts are even less known around 3.0 GHz than around 300 MHz. Since Oct. 1996, a spectrometer with high time and frequency resolution at the Beijing Astronomical Observatory (BAO) has been recording solar bursts in the frequency range 2.60–3.80 GHz. The first event with complicated fine structures was recorded on Apr. 15 1998.

We will emphasise three special fine structures of a kind that we had never recorded before in such a high frequency range (around 3.60 GHz). We will discuss these features in relation to previously identified structures at lower frequencies (around 300 MHz), such as the "zebra patterns" and the "evolving emission line" (EEL) reported by Chernov et al. in 1998.

In Sect. 2, we will describe the instrument and the main features of the event. In Sect. 3, we will analyse and properties of three fine strutures. In Sect. 4, we will discuss what they might be. We will conclude in Sect. 5.

Send offprint requests to: Zongjun Ning

2. Observation

For a detailed study of fine structures in the high-frequency part of decimetric and microwave bursts, new spectral observations (intensity and polarization) with high resolution in time and in frequency over a wide frequency range are needed. For this purpose, a broad band radio spectrometer is being developed by the solar radio astronomical community of China (Fu et al. 1995). It is composed of five separate spectrometers covering the respective frequency ranges: 0.70–1.40 GHz, 1.00–2.00 GHz, 2.60–3.80 GHz, 4.00–5.20 GHz and 5.20–7.60 GHz. The 2.60–3.80 GHz component spectrometer started working in Oct. 1996 at BAO; it has 120 frequency channels of 10 MHz bandwidth each, a time resolution of 8 milliseconds, as well as allowing high sensitivity and high accuracy measurement of circular polarization (Ji et al. 2000).

An overview of solar radio bursts on Apr. 15 1998 observed by BAO over the band 2.60–3.80 GHz is given in Fig. 1, including the left- and right-handed circular dynamic spectrum and polarization; the data is integrated into a time resolution of 200 ms. There is a decimetric pulsation (DCIM) event between 0741 UT and 0749 UT, and about 9 minutes later, from 0758 UT to 0815 UT, a second DCIM was observed. On the rising phase of the second DCIM emission, from about 0747 UT to 0802 UT, various fine structures are detected, thanks to the high time and frequency resolution. Three of these structures are given in Fig. 2a–c (FS a, FS b, and FS c in chronological order respectively) with a right-handed circular component. FS b and FS c are very close to each other, however, there are other kinds of fine structures between FS a and FS b.

These two DCIM were also recorded by the spectrometer over a range from 2000 MHz to 4395 MHz at the Ondrejov Observatory (ONDR). On the other hand, Solar Geophysical Data (SGD) reports a C8.8/SN flare detected by GOES and SVTO in active region(AR) 8203 located at N29W15; the flare occurred from 0737 UT to 0806 UT, reaching its maximum at 0746 UT. Therefor, AR 8203 and its flare are the likely source of the two DCIM events as the optical emssion begins slightly before the radio emission. In the observations of YOHKOH, a small arcade structure is detected in the soft X-ray (SXR) in AR 8203 between 0806 UT and 0816 UT. However, the hard

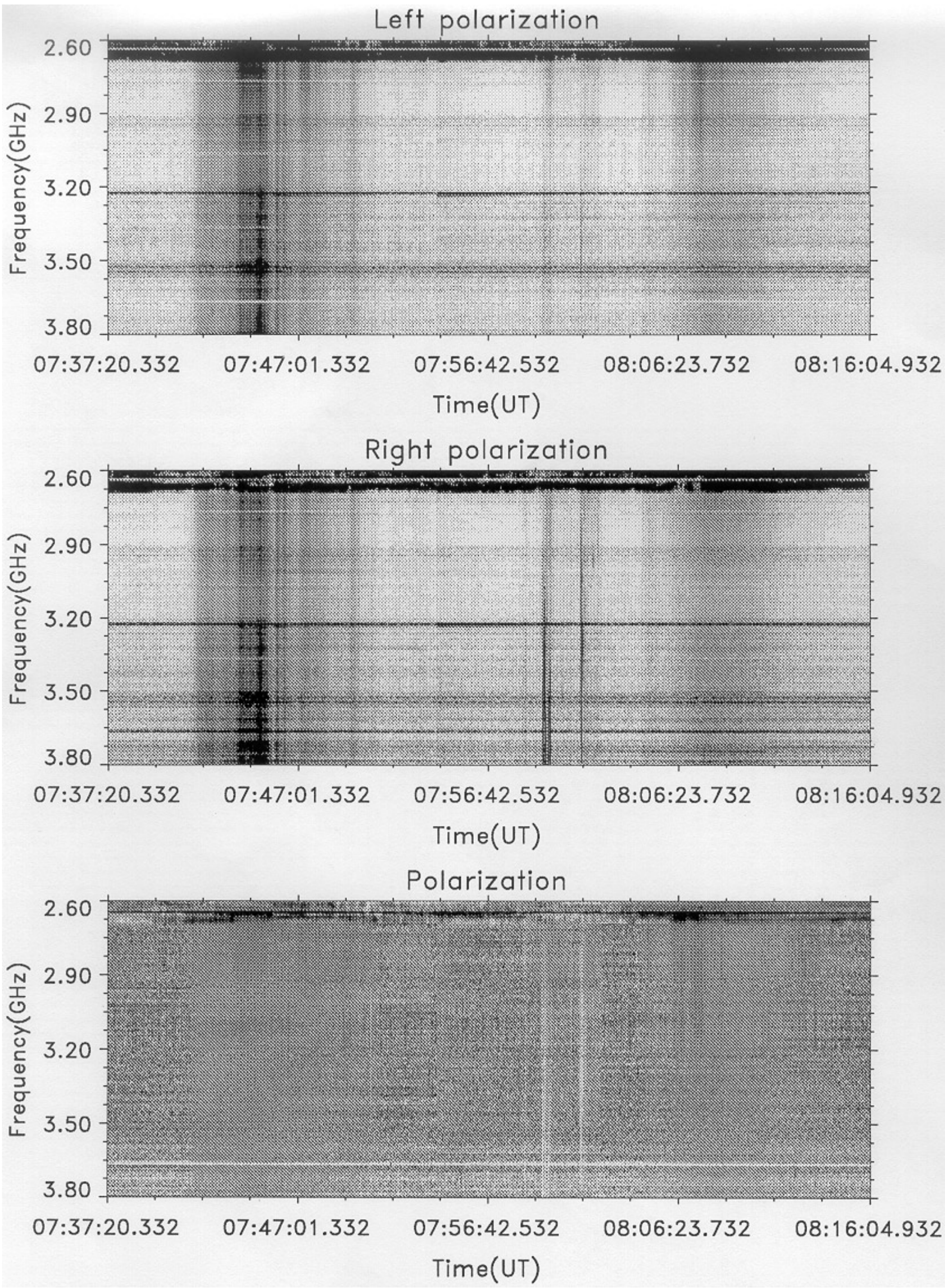

Fig. 1. Dynamic spectrum of the DCIM on April 15 1998 observed by the BAO spectrometer in the 2.60–3.80 GHz band. From top to bottom: left- and right-handed circular components and polarization degree respectively. The data is integrated into the time resolution of 200 ms. The first triangle corresponds to the FS a in Fig. 2, and the second one indicates the FS b and c (the two are very close to each other).

X-ray event (HXR) recorded by BATSE on channel 0 (33.2–56.9KeV) lasts from 0740 UT to 0752 UT. In addition, there are also coronal mass ejection (CME) events by SOHO and type II bursts on Apr. 15–18 1998.

3. Data analysis

As shown in Fig. 1, the first DCIM has a constant average circular polarization of 3% left-handed. However, the second DCIM changed polarization from –80% right-handed during the rising phase to 14% during the decay phase. Fine structures appear at the beginning during the high polarization phase: spike groups, pulsations, patch and zebra pattern or EEL(FS a, FS b, FS c). We now describe three characteristic fine structures in detail.

3.1. FS a

FS a in Fig. 2a is composed of a continuum on the lower frequency part and two narrow band emissions on the higher frequency part. It is unfortunate that only a part of FS a was recorded, since as it is clear that it continues beyond the 3.80 GHz high frequency limit of the spectrometer, so we do not know exactly what its bandwidth and duration are. However, we can state the following:

(1) FS a has a duration of more than 1 s;
(2) FS a occurs in the range 2.84 GHz–$\geq$ 3.80 GHz;
(3) In the low frequency range from 2.84 GHz to 3.67 GHz, there is a weaker continuum from the beginning to the end;
(4) In the high frequency range from about 3.67 GHz to 3.80 GHz, two narrow band emissions are present, with band-

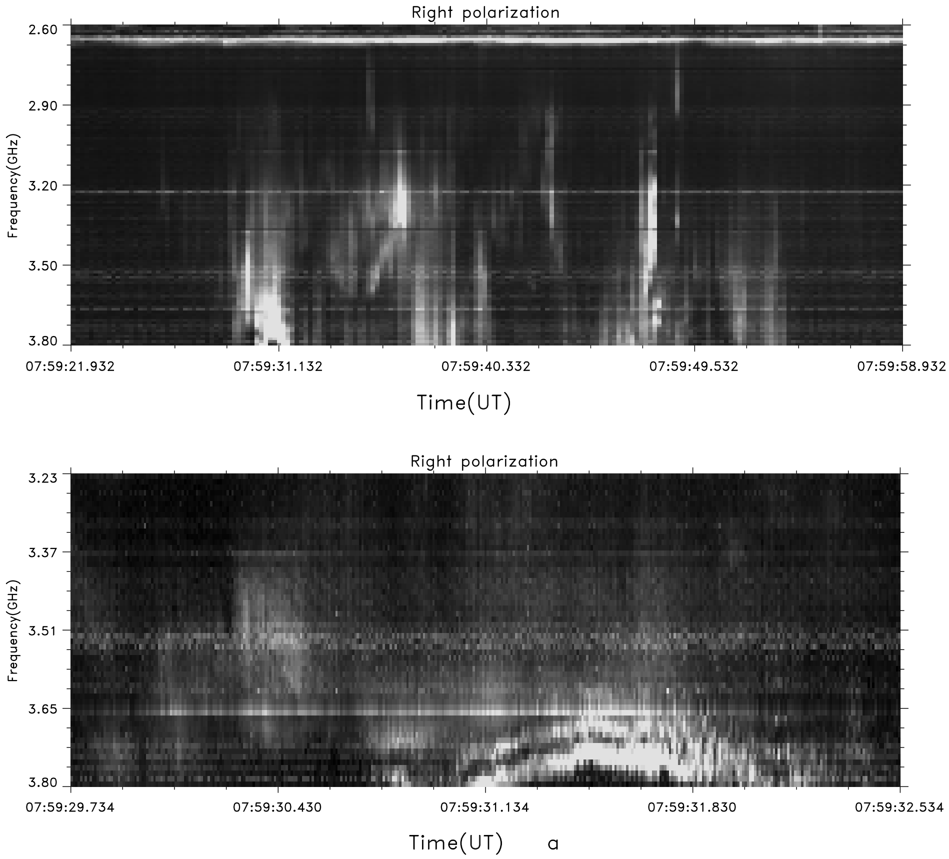

Fig. 2a. Three special fine structures in the rising phase of the second DCIM around the time 1998 0415 0800 UT. FS a, b and c (the data with a time resolution of 8 ms) are three EEL events, the other two pictures have a time resolution of 200 ms. The triangle marker in FS b points to the period where five strips are split during 84 ms.

widths $\Delta f \simeq$ 10–20 MHz and 40 MHz for the top (lowest frequency) and bottom (highest frequency) respectively. The corresponding relative bandwidths are $\Delta f/f \simeq$0.004 and 0.011. The frequency separation between the two strips decreases from about 20 MHz at the beginning to zero at the end when they merge into a single strip. The central frequencies of either strip decrease and then increase again simultaneously by about 100 MHz, over the 1 s time period during which we observed them. This corresponds to a relative frequency variation $\delta f/f \simeq$0.03 which could be due to either a plasma density variation $\delta n_e/n_e \simeq 2\delta f/f \sim$0.07 (plasma emission), or to a magnetic field variation $\delta B/B = \delta f/f \sim$ 0.03 (electron-cyclotron emission);

(5) FS a keeps the same sense and high degree of polarization all the time (–80% right-handed).

3.2. FS b

This is the most complicated of the three recorded, with lots of detail; it is similar to the "evolving emission line" (EEL) described by Chernov et al. (1998). A pulsating continuum predominates at lower frequencies, and two or three narrow band emissions occur on the high frequency part.

(1) FS b lasts for more than 4 s;

(2) FS b ranges over slightly more than 1.00 GHz bandwidth from 2.72 GHz to 3.78 GHz;

(3) The low frequency continuum is modulated by quasi-periodic pulsations. The intensity fluctuation is given in Fig. 3; we identify a quasi-period of about 275 ms, compared to the continuum pulsation period of 3 minutes at 300 MHz in Chernov et al.'s event. The continuum becomes weaker and weaker from high to low frequencies;

(4) From the beginning to 0801 28.4. UT, two narrow band emissions on the high frequency part, 10–20 MHz wide and 10–20 MHz apart, wiggle by about 50 MHz. At $\sim$ 0801 28.5. UT (solid triangle marker), and for about 0.1 s, the whole emission splits into five narrow bands, 20 MHz wide and about 10 MHz apart; during this short period, the low frequency part of the continuum is much weaker than nearby. Right afterwards the spectrum is smooth, and about 0.3 s later, at 0801 28.8. UT, the bursts split into three narrow band emissions again, about 30 MHz wide (bottom strip) to about 50 MHz wide (top), corresponding to relative bandwidths $\Delta f/f \simeq$ 0.004 to 0.01 respectively. The frequency separation is about 20 MHz. These three strips synchronously wiggle by about 200 MHz on a time scale of 0.5 s – the relative frequency variations $\delta f/f \simeq$ 0.06 corresponds to a plasma density variation $\delta n_e/n_e \sim$0.1 or to a magnetic field variation $\delta B/B \sim$0.06;

(5) FS b has the same sense and degree of polarization as FS a.

3.3. FS c

(1) We have recorded all of this fine structure, which closely follows FS b; the duration is less than 1 s;

(2) The bandwidth is less than 800 MHz;

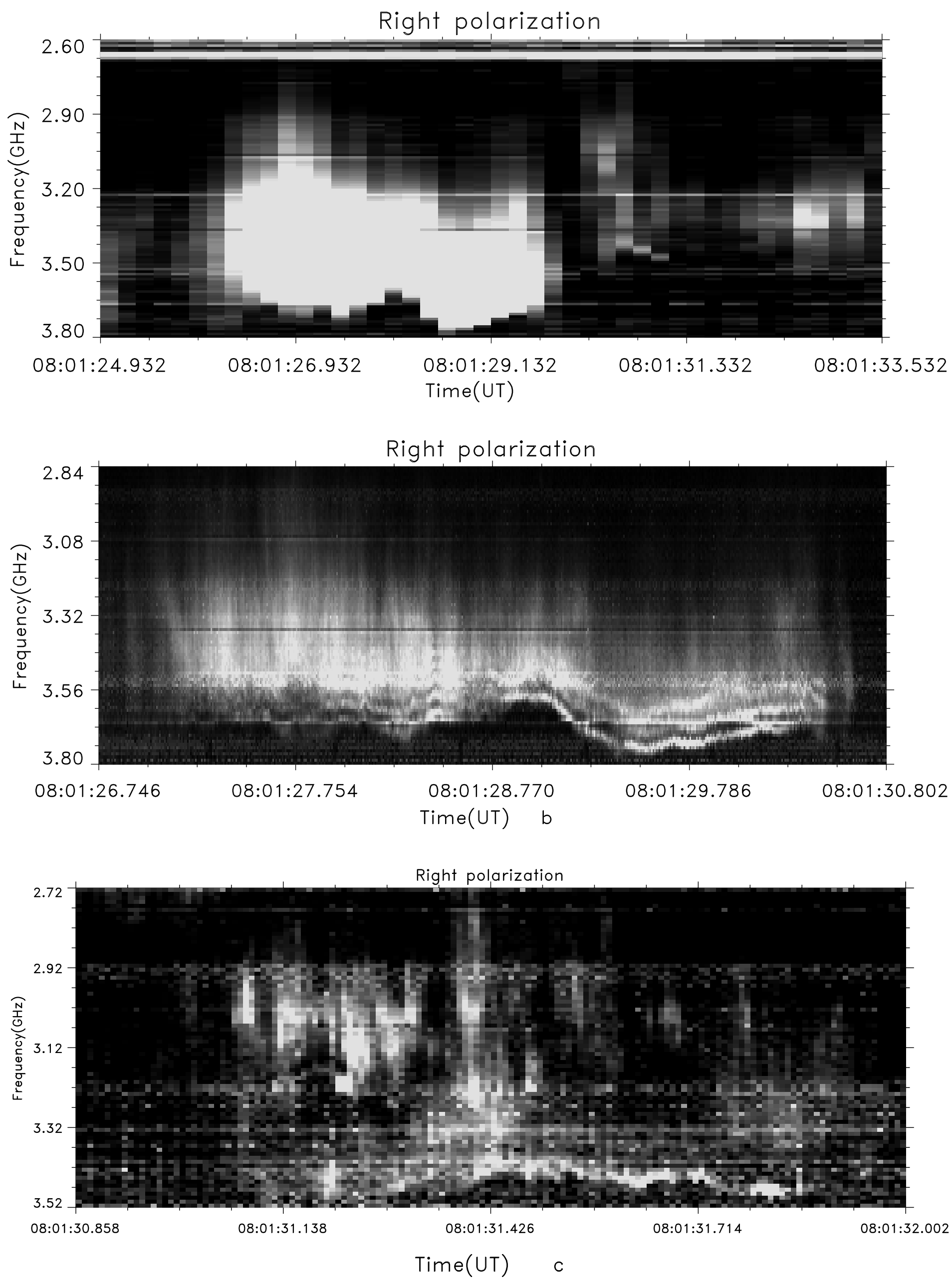

Fig. 2b and c.

(3) Instead of a continuum, the low frequency part consists of spikes from 2.70 GHz to 3.40 GHz: durations ≈ 24–40 ms, bandwidth ≈ 40–110 MHz (Isliker & Benz 1994);

(4) A narrow band emission, about 10 MHz wide, is cut off on the high frequency part and wiggles by about 80 MHz (from 3.41 GHz to 3.49 GHz) on a time scale of one second;

(5) The sense and degree of polarization stay the same during the recording, as in FS a and b.

4. Discussion

The dynamic spectra shown on Fig. 2a–c are reminiscent of the "zebra pattern" seen in type IV bursts or evolving emission lines (EELs).

4.1. zebra pattern

Zebra patterns are characterised by a number of simultaneous emission strips; the strip bandwidth is narrower than the frequency separation, both being about uniform across the different strips. The strip central frequencies fluctuate in parallel on a typical time scale of a few seconds. The emission strips are usually considered to be harmonics sω_f of a fundamental frequency ω_f, where s represents consecutive integers. Such features as band splitting, strip wiggling and strip disappearance occur occasionally (Kuijpers 1975; Chernov et al. 1998).

4.2. EEL

The EEL event was firstly reported by Chernov et al. (1998) around 300 MHz. They describe it as "right along the high-

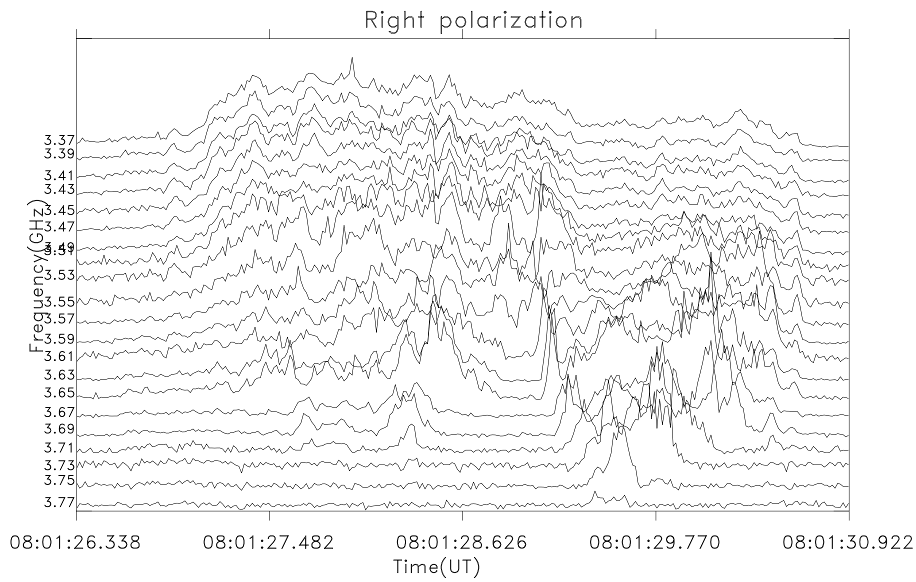

Fig. 3. Time profiles on selected channels on the low frequency part in the FS b. Notice the quasi-periodic pulsations with an average of about 275 ms.

frequency cut-off line of the pulsating continuum, and following its frequency fluctuations, a narrow band emission, 10–15 MHz wide, oscillates almost sinusoidally in frequency". In addition, the EEL consists of absorption (white) and emission (black) dots with 0.25 s period; Chernov et al. think that the absorption dots result from the quenching of loss-cone instability when new particles are injected inside the current sheet. Because of the EEL being at the highest frequency emitted, it is tempting to locate its source in the densest part of the whole radiating volume, that is inside the current sheet where magnetic reconnection proceeds.

4.3. Difference between zebra pattern and the EEL

Chernov et al. think there are three differences between them:

(1) The EEL mostly consists of one single emission band instead of many in zebra patterns;
(2) The EEL has a larger relative bandwidth than zebra patterns;
(3) It is continuous instead of intermittent.

Moreover, in zebra patterns the frequency separation between strips is larger than the strip bandwidth, and strips wiggle over a frequency interval comparable to the frequency separation between them. In addition, the EEL is right along the high-frequency cut-off line, which results from its source being located in the densest part of the whole radiating volume.

4.4. Our viewpoint

Firstly, we think the FS a is not the zebra pattern at 3.60 GHz because:

(1) The two strips have different bandwidth, 10–20 MHz for the upper and 40 MHz for the lower strip;
(2) The intensity of the lower strip is larger than that of the upper one;
(3) There is some weaker continuum on the low frequency part;
(4) Sometimes during the course of the zebra pattern, one zebra strip disappears while the neighbours approach each other and continue (Kuijpers 1975); however, in FS a, no strip disappears, but two strips combine together at the end;
(5) The strips wiggle by about 130 MHz, much more than the frequency separation between them;
(6) The frequency separation between two strips, which is equal to or smaller than the strip emission band, is changing, from 20 MHz at the beginning to zero at the end.

Although we do not know what zebra pattern could look like around 3.60 GHz, the features above are different from zebra strips around 200–300 MHz. In the event that the FS a was a zebra pattern, we presume that the fundamental frequency would be about 20 MHz (the frequency separation between them), so the same strip emission would have to continuously change its harmonic number s from 190 through 184 to 190 with time, when the strip wiggles from 3.80 GHz through 3.67 GHz to 3.80 GHz again. Therefore, although we also do not know what FS a looks like at frequencies higher than 3.80 GHz, we conclude it is of the EEL kind.

Secondly, the FS b is an EEL with some new properties around 3.60 GHz. The reasons are:

(1) It has a narrow cut-off strip emission at the high frequency all the time, which is the most important reason;
(2) The continuum is modulated with a quasi-period of about 275 ms on the low frequency part;
(3) The three strip emissions have different bandwidth (30 MHz to 50 MHz).

On the other hand, the FS b also has some new features:

(I) The bursts split into five narrow band emissions for 84 ms and then these five strips combine together and finally split into three line emissions again;
(II) The three strips synchronously wiggle by about 200 MHz on a time scale of 500 ms, which is much larger than the frequency separation (20 MHz) among them;

(III) The line emission is continuous with no absorption dots.
(IV) The lines have a pseudo-period of their frequency fluctuations, which is about 2 s.

The 5 strips lasting 84 ms are somewhat similar to a short portion of the zebra patterns recorded at lower frequencies. But they are not zebra pattern because the emission band (about 20 MHz) is larger than frequency separation (about 10 MHz). This is also the main reason why the following three line emissions are not zebra strips.

Thirdly, FS c is also an EEL event, since it is right along the high-frequency cut-off line. However, some spike groups on the low frequency part are new features of the FS c.

Finally, we conclude FS a, b and c are EEL events around 3.60 GHz.

5. Conclusion

Type IV solar radio bursts exhibit a wealth of well-documented fine structures between 100 MHz and 1 GHz. The BAO radiospectrograph aims to carry out high time and frequency observations at higher frequencies where fine structures are still poorly known. In this paper, we have reported an observation by this instrument of a short type IV-DCIM burst lasting 3 minutes, between 3 and 4 GHz.

This event exhibits remarkable fine structures which do not seem to be related to zebra-patterns, but rather to the EEL reported by Chernov et al. (1998). We describe in detail three characteristic phases where the EEL is clearly visible as one, two or three simultaneous emission strips, whose frequencies fluctuate in parallel at the high frequency limit of the event.

EELs are the only example of a narrow, isolated and continuous emission line in solar radio bursts. Such a spectral line is potentially rich in information on the physical parameters inside the radiation source. It may deserve substantial theoretical attention. A major question to be solved in the future is whether an EEL is the signature of a current sheet. Another question is why is this kind of feature so rare; is it because emission lines are usually too wide to show up as such, or is it because the emission mechanism itself requires a specific and narrow range of local parameters? We will also have to eliminate the remote possibility that such fine structures are the result of propagation effects through the inhomogeneous corona. The final question is to judge the possible continuity among all the fine structures on that day, including the 3 EELs in Fig. 2.

The present observation constitutes the second detection of an EEL, and the first one at frequencies higher than 1 GHz. It gives us the incentive to look for more EEL examples, throughout a wide possible frequency range, between approximately 100 MHz and 10 GHz. We need to get a statistical idea of its properties: frequency of occurrence, distribution in frequency, association with emissions at other wavelengths, etc.

Acknowledgements. It is a pleasure to thank Dr. Debang Lao and Dr. Guo Yang for supplying us with IDL software for analyzing the data; we also thank the staff of the BAO for providing help to complete this paper. This work is supported by National Nature Science Foundation project No. 19773016 and 19833050. We also appreciate Dr. M.Poquerusse spending plenty of time to improve this paper.

References

Chernov G.P., Markeev A.K., Poquerusse M., et al., 1998, A&A 334, 314
Fu Q., Qin Z., Ji H., Pei L., 1995, Solar Phys. 160, 97
Isliker H., Benz A.O., 1994, A&AS 104, 145
Ji H.R., Fu Q.J., Liu Y.Y., et al., 2000, ACTA Astronphysica Sinica Vol.20, No.2, 209
Kuijpers J., 1975, A&A 40, 405